Conserved features of intermediates in amyloid assembly determine their benign or toxic states

Rajaraman Krishnan[a,1,2], Jessica L. Goodman[a,1], Samrat Mukhopadhyay[b,1,3], Chris D. Pacheco[a,4], Edward A. Lemke[b,5], Ashok A. Deniz[b,6], and Susan Lindquist[a,c,6]

[a]Whitehead Institute for Biomedical Research, Cambridge, MA 02142; [b]Department of Molecular Biology, The Scripps Research Institute, La Jolla, CA 92037; and [c]Department of Biology, Howard Hughes Medical Institute, Massachusetts Institute of Technology, Cambridge, MA 02139

Contributed by Susan Lindquist, June 5, 2012 (sent for review December 21, 2011)

Some amyloid-forming polypeptides are associated with devastating human diseases and others provide important biological functions. For both, oligomeric intermediates appear during amyloid assembly. Currently we have few tools for characterizing these conformationally labile intermediates and discerning what governs their benign versus toxic states. Here, we examine intermediates in the assembly of a normal, functional amyloid, the prion-determining region of yeast Sup35 (NM). During assembly, NM formed a variety of oligomers with different sizes and conformation-specific antibody reactivities. Earlier oligomers were less compact and reacted with the conformational antibody A11. More mature oligomers were more compact and reacted with conformational antibody OC. We found we could arrest NM in either of these two distinct oligomeric states with small molecules or crosslinking. The A11-reactive oligomers were more hydrophobic (as measured by Nile Red binding) and were highly toxic to neuronal cells, while OC-reactive oligomers were less hydrophobic and were not toxic. The A11 and OC antibodies were originally raised against oligomers of Aβ, an amyloidogenic peptide implicated in Alzheimer's disease (AD) that is completely unrelated to NM in sequence. Thus, this natural yeast prion samples two conformational states similar to those sampled by Aβ, and when assembly stalls at one of these two states, but not the other, it becomes extremely toxic. Our results have implications for selective pressures operating on the evolution of amyloid folds across a billion years of evolution. Understanding the features that govern such conformational transitions will shed light on human disease and evolution alike.

Various oligomeric and prefibrillar species associated with the formation of amyloids have been known for many years (1–3). Experiments with the prion-determining region of the yeast Sup35 protein first established that a small, conformationally-molten, oligomeric species was a critical obligate, on-pathway intermediate in amyloid assembly (4, 5). This fact was later confirmed for several other amyloidogenic polypeptides, including those involved in diseases, functional amyloids, and protein fragments of diverse origins (6). Most of these oligomeric polypeptides transition through a variety of prefibrillar forms before reaching the final stable amyloid state (2, 3).

Interest in oligomeric intermediates increased when it was realized that oligomers of the β-amyloid peptide (Aβ), the polypeptide implicated in Alzheimer's disease, kill neurons and inhibit hippocampal long-term potentiation (7, 8). Surprisingly, despite great diversity in primary amino-acid sequences, the oligomers of very different amyloidogenic proteins appear to elicit toxicity by a common mechanism (6). This toxicity involves membrane perturbations, calcium dysregulation, the accumulation of reactive oxygen species, and the activation of apoptotic signaling pathways (9–11). It has also become clear that these amyloidogenic polypeptides can populate oligomeric states that are not toxic (1, 12, 13). Unfortunately, the heterogeneity and unstable nature of these naturally occurring oligomeric intermediates make it difficult to define their conformational transitions and discern the physio-chemical properties that correlate with toxicity. Here, we take advantage of tools developed for diverse amyloidogenic polypeptides, as well as tools developed specifically for the Sup35 protein, to investigate these questions.

The yeast Sup35 protein is intensely studied, both because it provides a model for amyloid formation and because the self-templating amyloid it forms serves as a remarkable "protein-only" element of inheritance (4). Such elements are known as yeast prions (14). In its normal soluble, non-prion form, [psi^-], Sup35 acts as a translation-termination factor. In its prion state, [PSI^+], Sup35 is sequestered into amyloid. Neither the soluble nor the amyloid form of Sup35 is toxic per se (14). However, sequestration into amyloid reduces translation termination efficiency. This creates a host of new traits that can be detrimental or beneficial depending upon the particular growth environment (15). Indeed, [PSI^+] and other yeast prions are widely deployed by wild yeasts to create phenotypic diversity. The inheritance of these prions might constitute an important evolutionary mechanism for survival in fluctuating environments (14–16). Two conserved features of yeast prion biology ensure the inheritance of prion-based traits. First, the prion amyloid conformation, once acquired, is efficiently self-templating (4). Second, the protein remodeling factor Hsp104 fragments the amyloid template to ensure faithful inheritance from mother cell to their daughters (14).

The Sup35's prion-determining region (NM) contains two subdomains that allow it to exist as either a soluble functional translation factor or an insoluble amyloid. The N-terminal subdomain (N; residues 1–123) is highly enriched in the uncharged polar amino acids glutamine and asparagine and is very amyloidogenic (14). The Middle subdomain (M; residues 124–253) is highly charged and confers solubility (14). In vitro, when NM is diluted from denaturant into buffer, it initially remains soluble and intrinsically disordered. It then converts into oligomeric species and, finally, assembles into amyloid (4). The ability of very low concentrations of an oligomer-specific antibody, A11, to block assembly established that this particular oligomeric species is an obligate, on-pathway intermediate in assembly (5).

The antibody A11 was originally raised against an oligomeric species of Aβ (17). The primary amino-acid sequence of NM

Author contributions: R.K., S.M., C.D.P., A.A.D., and S.L. designed research; R.K., J.L.G., S.M., C.D.P., and E.A.L. performed research; S.M., E.A.L., and A.A.D. contributed new reagents/analytic tools; R.K., J.L.G., S.M., C.D.P., E.A.L., A.A.D., and S.L. analyzed data; and R.K., J.L.G., and S.L. wrote the paper.

The authors declare no conflict of interest.

[1]R.K., J.L.G., and S.M. contributed equally to this work.

[2]Present address: Neurophage Pharmaceuticals, 222 Third Street, Suite 3120, Cambridge, MA 02142.

[3]Present address: Departments of Biological Sciences and Chemical Sciences, Indian Institute of Science Education and Research (IISER), Mohali 140306, India.

[4]Present address: HighRes Biosolutions, 299 Washington Street, Woburn, MA 01801.

[5]Present address: European Molecular Biology Laboratories, Meyerhofstraβe 1, 69117 Heidelberg, Germany.

[6]To whom correspondence may be addressed. E-mail: deniz@scripps.edu or lindquist_admin@wi.mit.edu.

This article contains supporting information online at www.pnas.org/lookup/suppl/doi:10.1073/pnas.1209527109/-/DCSupplemental.

is completely different from that of Aβ. Yet A11 reacts with oligomeric forms of both proteins. It recognizes neither their monomeric nor their amyloid forms (5, 17). The antibody A11 also reacts with oligomeric forms of many other unrelated amyloidogenic peptides, establishing it as a conformation-specific antibody (17).

Oligomers that are A11-reactive are only a subset of a diverse population of oligomeric species that form during amyloid assembly, which are highly dynamic in character. Methods for characterizing these species and determining their biological properties are sorely lacking. Here, we use a combination of approaches to further define features of NM oligomers that form during normal assembly. We employ several methods to inhibit assembly at specific oligomeric stages and characterize the physical properties of arrested species. Finally, we evaluate their toxicity to neuroblastoma cells.

Results

Labeling NM With Fluorescent Probes Doesn't Perturb Amyloid Assembly or Structure. As an initial tool we used NM proteins labeled with a variety of fluorescent probes (Alexa-488, Cy3B, or Cy5). Since NM naturally contains no cysteines, we employed a site-specific glutamine-to-cysteine substitution, Q38C, to attach these labels. Evidence from several laboratories indicates that residue 38 is in a critical region for NM amyloid conversion (18), putting it in an excellent position to report on conformational changes. We previously reported that when Q38C is used to replace wild-type Sup35 in vivo, it retains its ability to support both the prion and non-prion states (18). Moreover, in the presence of excess wild-type protein in vitro, Q38C labeled with Alexa-488 assembles with normal kinetics (18). Before employing Q38C-labeled proteins in further analyses, we sought to more rigorously determine whether fluorescent labels at this position alter normal amyloid assembly. To do so, we took advantage of the fact that NM assembles into different amyloid variants, with distinct physical and biological properties, when assembly is performed at 25 °C vs 4 °C (18).

Providing physical measures for amyloid variant type, these variants polymerize at different rates and denature at different concentrations of guanidinium chloride (GdmCl) (18). We allowed proteins labeled with Alexa-488, Cy3B, or Cy5 to assemble spontaneously with a large excess of wild-type NM at either 25 °C or 4 °C. In these reactions, Thioflavin-T (ThT) binding reported on the assembly of bulk protein and fluorescence anisotropy reported on the assembly of the fluorescent species. At each temperature, fluorescent proteins assembled with the same kinetics as the unlabeled proteins in the same reaction mixture (Fig. 1 *A* and *B* and Fig. S1). Furthermore, once assembled into trace-labeled fibers, the fluorescent protein and the bulk unlabeled protein exhibited the same GdmCl denaturation profile (Fig. 1*C* and Fig. S2).

The biological assay for NM amyloid variant type employs NM protein fibers to heritably "transform" [*psi*$^-$] cells to the [*PSI*$^+$] state. Different variants sequester different amounts of Sup35 protein into amyloid in vivo. The resulting differences in translation create heritable differences in colony color (14). Fibers assembled at 4 °C favor the formation of white colonies; fibers assembled at 25 °C favor the formation of pink colonies. We transformed [*psi*$^-$] cells with the trace-labeled fibers described above. Three independent transformations were performed with eight different fiber preparations: unlabeled fibers and fibers trace-labeled with each of the three fluorophores, assembled at either 4 °C or 25 °C. From each transformation, 50 colonies were selected and replated to score for colony color. Each of the trace-labeled fibers produced the same distribution of white vs pink colonies as completely unlabeled fibers assembled at the same temperature (Fig. 1 *D* and *E*). Taken together, these in vitro and in vivo analyses establish that small amounts of fluorescently labeled-NM do not perturb the conformational transitions of NM monomers into amyloid.

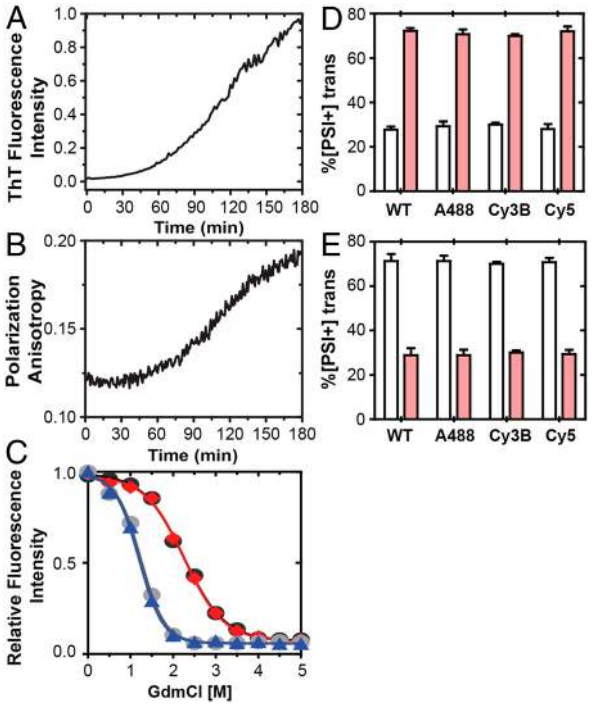

Fig. 1. Probing assembly of oligomers during lag phase. (*A*) Assembly kinetics of NM mixed with trace amounts of Alexa-488 Q38C by ThT fluorescence. (*B*) Polarization anisotropy kinetics of NM mixed with trace amounts of Alexa-488 Q38C under identical conditions. (*C*) GdmCl-mediated disassembly of fibers monitored by ThT fluorescence. Disassembly of unlabeled fibers assembled at 25 °C (black circle) and at 4 °C (gray circle), and of fibers trace-labeled with Alexa-488 assembled at 25 °C (red diamond) and 4 °C (blue triangle). (*D*, *E*) Yeast transformed with either unlabeled fibers (WT), or fibers trace-labeled with Alexa-488 (A488), Cy3B or Cy5 assembled at either (*D*) 25 °C or (*E*) 4 °C were categorized by prion strains based on colony color. White bars represent the number of colonies that scored as white prion strains; pink bars represent colonies that scored as pink prion strains. Data are shown as mean ± SEM ($n = 3$).

Probing Oligomeric NM Intermediates by Single Molecule Fluorescence Anisotropy. Having demonstrated that these three fluorescent labels do not perturb normal NM assembly, we employed them to investigate the transient oligomeric intermediates that form during this process. First, we took advantage of recent developments in single-molecule technology that allow the fluorescence anisotropy of individual molecular species to be determined in real time. The anisotropy of a fluorophore-labeled protein is related to its rotational correlation time, which, in turn, is proportional to the third power of its hydrodynamic radius (19). This provides an extremely sensitive measure of size (20). Using a home-built laser confocal microscope with a polarizing beam-splitter, we assessed the anisotropy of hundreds of individual molecules. At the protein concentrations we employed, the laser-illuminated confocal detection volume was small enough to ensure that most of the time no fluorescent molecules were in the field. Thus, each fluorescent burst represented an individual molecular species passing through this volume. Parallel and perpendicular polarized photons were separated and the distribution of fluorescent intensities and anisotropies were calculated from hundreds of collected fluorescent bursts.

Our previous single molecule fluorescence resonance energy transfer and fluorescence correlation spectroscopy studies established that NM remains monomeric when it is maintained at low concentrations (100 pM), populating an ensemble of rapidly fluctuating compact conformational states (21). The single molecule anisotropy measurements performed here, at these same concentrations, revealed a similar distribution of monomeric species with an r-value that peaked at approximately 0.1 (Fig. 2*A*). Shortly after mixing with a large excess of unlabeled NM, the

distribution shifted to a higher anisotropy value (approximately 0.16; Fig. 2*B*). This shift, and the additional broadening of the distribution, can be attributed to the rapid formation of oligomeric species. At the end of the lag phase, the histogram showed an altered population distribution, with low and high anisotropy peaks, suggesting the presence of relatively stable multimeric species (Fig. 2*C*).

Oligomers Conformationally Mature During the Lag Phase. Next, with Cy3B-labeled NM, we used ensemble fluorescence measurements and tyrosine quenching to report on changes in the environment of residue 38 during oligomer maturation. The Cy3B fluorescence is highly susceptible to quenching by aromatic amino acids (22). We have previously taken advantage of quenching by the large number of tyrosine residues in the N subdomain of NM (20 of 123 residues) to monitor conformational dynamics of fluorescently-labeled NM monomers (21). Here, we employed tyrosine quenching to assess conformational rearrangements of oligomeric intermediates during assembly. We monitored both parallel and perpendicular components of Cy3B emission (Fig. S3). From each set of kinetic data, we constructed time courses both for fluorescence intensity and for anisotropy (Fig. 3*A* and *SI Text*, Eqs. **S1** and **S2**). These two measurements enabled simultaneous assessment of changes in oligomer sizes and conformations.

To determine the kinetics of amyloid assembly under these conditions, reactions of unlabeled proteins and of proteins trace-labeled with Cy3B were monitored with ThT (Fig. S4). For both reactions, the lag phase for amyloid formation was 105 ± 2 min (Fig. S4). During the initial half of this lag phase, the fluorescent intensity of the Cy3B label remained high (Fig. 3*A*, red trace). Fluorescence intensity then abruptly decreased, indicating that the tyrosines reorganized to produce high quenching at residue 38. Finally, during the amyloid assembly phase, fluorescence intensity partially recovered, indicating that the tyrosine residues reorganized again, becoming more spatially segregated from the Cy3B label in the final amyloid fiber.

Looking at anisotropy with the Cy3B label, we observed the expected increase during the amyloid assembly phase, commensurate with the formation of larger species (Fig. 3*A*, blue trace). However, starting about halfway through the lag phase we consistently observed a small but reproducible drop in anisotropy (Fig. 3*A*, blue trace, starting around 75 min). This result suggested that, before assembly, there was a decrease in the number of monomers per oligomer and/or that the oligomers rearranged to become smaller and more compact in size, thereby increasing the rate of tumbling. However, anisotropy is dependent not only on molecular size but also on fluorescent lifetime. Because tyrosine quenching reduces the fluorescence lifetime of Cy3B, changes in size can be obscured. Therefore, we turned to another label not affected by tyrosine quenching, Cy5, to more clearly assess the potential change in oligomer size by anisotropy (22).

The Cy5-labeled NM showed an even larger drop in anisotropy during the second half of the lag phase (Fig. 3*B*). Thus, the oligomers that had formed early in assembly were transformed into a distinct species prior to amyloid assembly. Specifically, tyrosines rearranged (as reported by Cy3B) and the oligomers become smaller and/or more compact (as reported by Cy3B, and even more accurately by Cy5). Together, these findings establish distinct kinetic phases in the lag phase of NM assembly.

Probing Assembly with Conformation-Specific Antibodies and Detergent Sensitivity. To provide an independent, label-free assessment of conformational transitions, we employed conformation-specific antibodies (1). Small amounts of spontaneous unlabeled NM assembly reactions were withdrawn at different times and spotted onto nitrocellulose membranes (Fig. 3*C*). The membranes were then probed with conformation-specific antibodies, as well as with a control antibody specific to the M subdomain (Fig. 3*C*, Anti-M).

The A11 antibody, which recognizes an oligomeric intermediate in Aβ assembly (17), also recognizes an oligomeric intermediate in NM assembly. As previously reported, this species peaks during the lag phase and quickly disappears during assembly (5) (Fig. 3*C*). Another conformation specific antibody, known as OC, recognizes Aβ oligomers and fibrils, as well as oligomers

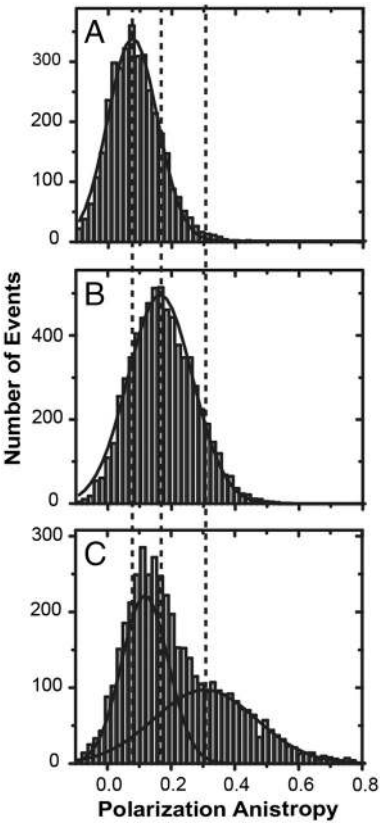

Fig. 2. NM assembly involves transitions through oligomeric species. Single-molecule fluorescence anisotropy histograms of 100 pM of Alexa-488 Q38C in refolding assembly buffer (*A*) under monomeric conditions, (*B*) in oligomeric form (5 min after mixing with excess NM), and (*C*) after the lag phase (1 h after mixing).

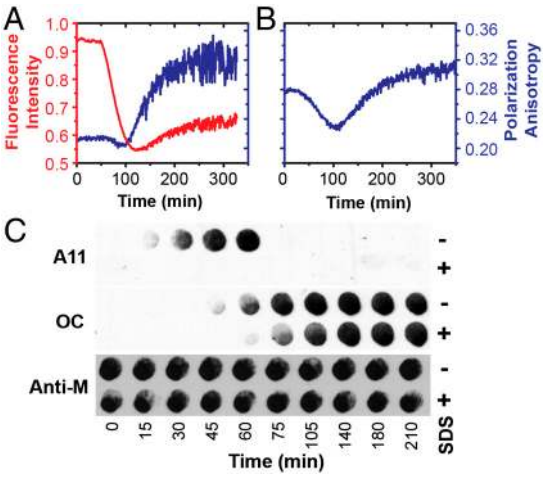

Fig. 3. Conformational and size changes of oligomers during assembly. (*A*) Fluorescence intensity (red, left axis) and anisotropy (blue, right axis) kinetics of 5 μM NM with 50 nM Cy3B Q38C. (*B*) Fluorescence anisotropy (blue, right axis) of 5 μM NM with 50 nM Cy5 Q38C. (*C*) Dot blot analysis of on-pathway oligomers formed during the assembly of 10 μM NM. These blots were probed with A11, OC, and Anti-M (Sup35) antibodies. Samples withdrawn at different time points were treated with SDS (+) or without SDS (–).

and fibrils of polyQ, IAPP and α-synuclein (23). Thus, like A11, OC recognizes a conformation common to diverse amyloid assemblies. However, this conformation is distinct from, and more mature than, that recognized by A11. OC's reactivity with NM has not been examined. We found that OC reacted with a species of NM that formed as the A11-reactive species disappeared (Fig. 3*C*).

Detergent sensitivity provides an independent measure of amyloid maturation. As for many other oligomers, molten oligomers of NM are sensitive to SDS, while NM amyloid fibers are not. To test the SDS sensitivity of these A11 and OC-reactive species, small aliquots of assembly reactions were incubated with 1% SDS before spotting to nitrocellulose. As expected, A11 oligomers were completely eliminated by SDS (Fig. 3*C*). Early OC-reactive species, formed near the end of the lag phase, were also SDS-sensitive. This sensitivity was lost later in assembly. Thus, the OC antibody is recognizing at least two distinct forms of NM, an oligomeric species more mature than the initial A11-reactive species, as well as an SDS-resistant mature amyloid.

As previously reported (5), A11 antibodies block NM assembly, even when present at very low concentrations relative to NM monomers [0.06 μM A11: 5 μM NM] (Fig. S5*A*). We found that OC antibodies had the same effect (Fig. S5*B*). However, OC was completely incapable of disassembling pre-formed NM fibers, even after two days of incubation with a five-fold higher concentration of the antibody (Fig. S5*C*). Thus, as is the case for the A11-reactive species, the early OC-reactive species is an obligate on-pathway conformer.

Structural Features of Oligomers Generated with Small Molecule Inhibitors. Small molecules can arrest the assembly of other amyloidogenic polypeptides (24). We tested four chemically diverse small molecules previously shown to inhibit the assembly of Aβ, α-synuclein, PrP, polyQ or insulin fibers (13, 24–26). All four compounds, amphotericin B (AmB), clotrimazole (CM), 4,5-dianilinophthalimide (DAPH1), and epigallocatechin gallate (EGCG), slowed NM assembly at a ratio of 1:2 compound:NM. They completely arrested assembly at a ratio of 4:1 (Fig. S6). We characterized these arrested species using the biophysical assays described above.

By monitoring the fluorescence intensity of Cy3B, each of the compounds slowed the maturation of oligomers into a state where fluorescence was quenched by proximal tyrosines (Fig. 4*A*; Table S1). Once this state was acquired, however, it was stable for days. Reorganization to the less quenched state that was associated with amyloid assembly never occurred (Table S1). Fluorescence anisotropy established that the sizes of these oligomeric species were also stable for days (Fig. 4*B*). After 48 h anisotropy values for NM complexes with AmB, CM, DAPH1, and EGCG were 0.32, 0.25, 0.3, and 0.33, respectively (Table S1).

Surprisingly, while the species stabilized by these compounds were indistinguishable by these biophysical measures, they had very different reactivities with conformation-specific antibodies. Oligomers formed with AmB and CM interacted strongly with A11 but not OC. Oligomers formed with DAPH1 or EGCG reacted with OC but not A11 (Fig. 4 *C* and *D*).

To further investigate oligomers stabilized by these compounds, we used the solvent-sensitive neutral dye, Nile Red. The spectral properties of Nile Red are unaffected by heavily charged regions in a protein (such as the M region of NM) or UV-absorbing aromatic compounds like AmB, CM, DAPH1, or EGCG (27). This dye has a low quantum yield in polar environments (emission maximum 655 nm) and its fluorescent intensity increases with a pronounced blue shift (maximum 625 nm) in apolar environments (27). Oligomers formed with all four compounds had blue-shifted Nile Red emission spectra (Fig. 4*E*), as did the spectra of mature fibers. However, the fluorescence intensities of oligomers arrested with AmB and CM were three- to six-fold higher than that of mature fibers. The fluorescence intensities of oligomers arrested with DAPH1 or EGCG were lower than that of mature fibers (Fig. 4*F*).

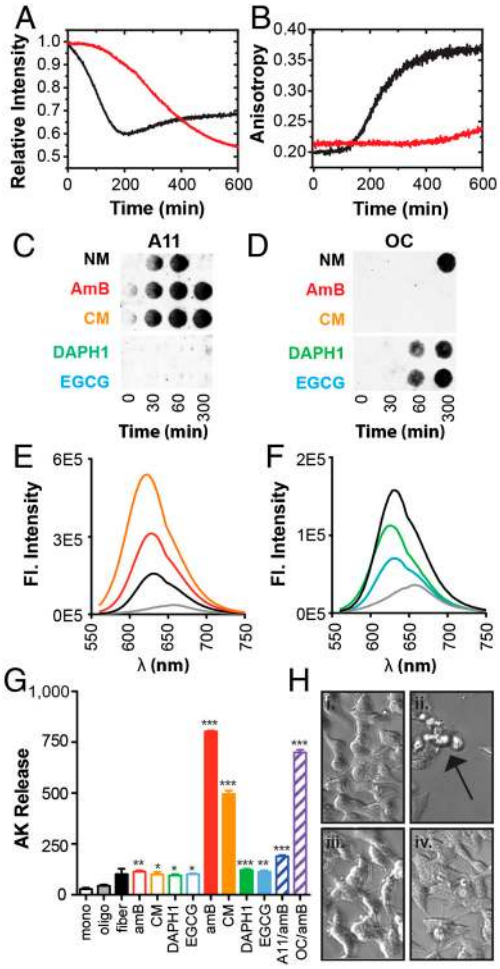

Fig. 4. Conformational properties of monomers, oligomers and amyloids. (*A*) Normalized fluorescence intensity of 5 μM NM with 50 nM Cy3B Q38C in the presence (-) or absence (-) of 10 μM AmB. (*B*) Fluorescence anisotropy of 5 μM NM with 50 nM Cy3B Q38C in the presence (-) or absence (-) of 10 μM AmB. (*C*, *D*) Dot blot analysis of NM-small molecule complexes probed with (*C*) A11 and (*D*) OC antibodies. (*E*, *F*) Nile red fluorescence emission spectra of 2.5 μM aqueous solutions of NM monomers (-), NM fibers (-) and complexes of NM with 10 μM solutions of AmB (-), CM (-), DAPH1 (-) and EGCG (-). (*G*) Toxicity of NM-small molecule oligomeric complexes (1.25 μM NM:5 μM compound) to SH-SY5Y cells as measured by adenylate kinase release. Compounds alone (empty bars), NM-compound oligomeric complexes (filled bars), or NM-compound oligomeric complexes neutralized with conformation specific antibodies (NM:antibody, 100:1, hatched bars). Data are shown as mean ± SEM ($n = 3$, *:$p < 0.05$; **:$p < 0.01$; ***:$p < 0.001$, Dunnett's test). (*H*) Images of SH-SY5Y cells incubated with compounds alone (i. AmB, iii. EGCG) or with NM-small molecule complexes (ii. AmB-NM, iv. EGCG-NM). Treatment with AmB-NM causes cell death (ii, black arrow).

(Note the change in scale for Fig. 4 *E* and *F*). Thus, the oligomers formed with DAPH1 and EGCG are more tightly packed with reduced exposure of hydrophobic surfaces than those formed with AmB and CM.

Oligomers Arrested with AmB or CM are Toxic. To investigate the toxicities of these NM species, we incubated them with adherent SH-SY5Y neuroblastoma cells. Toxicity was assessed by monitoring the release of adenylate kinase into the media (Fig. 4*G*), by propidium iodide staining (12 and Fig. S7), and by microscopic visualization (Fig. 4*H*). Monomeric NM, NM from various time points in assembly, and assembled NM fibers were not toxic. Oligomers arrested by EGCG and DAPH1 were also not toxic (Fig. 4 *G* and *H*). However, NM oligomers arrested by AmB or CM were severely toxic (Fig. 4 *G* and *H*).

A Conformation-Specific Antibody Eliminates the Toxic Species. These observations strongly suggested that AmB and CM arrest the normally non-toxic NM protein in a conformation that is both highly toxic and A11-reactive. However, the oligomers might simply "present" the compounds to cellular membranes in a manner that makes the compounds themselves toxic. To investigate, we asked whether the conformation-specific antibodies OC and A11 affected their toxicities.

Pre-incubating AmB-NM oligomers with OC antibodies had no effect on toxicity (Fig. 4*G*). However, even very low concentrations of A11 antibodies (NM:A11, 100:1) greatly reduced toxicity (Fig. 4*G*). Thus, the toxicity of oligomers arrested in an A11-reactive conformation by AmB and CM is due to a specific conformation of NM.

Oligomers Arrested in an A11-Reactive State by Crosslinking are also Toxic. Finally, we tested the toxicity of different oligomeric conformers of NM by two methods independent of small molecules. First, we took advantage of the many tyrosines in the amyloidogenic region of NM. NM monomers were exposed to UV light to form dityrosine crosslinks (9) (Fig. S8). The crosslinked oligomers were then separated into low molecular weight species (dimers and trimers) and higher molecular weight species in denaturant. Upon dilution into assembly buffer, both higher and lower molecular weight forms of NM were unable to assemble into fibers. The higher molecular-weight species retained a conformation that had low fluorescence with Nile Red (Fig. 5*A*) and reacted with OC antibody rather than with A11 (Fig. 5*B*). These species were not toxic to neuroblastoma cells (Fig. 5*C*). Lower molecular-weight species exhibited a high level of blue-shifted fluorescence with Nile Red (Fig. 5*A*) and reacted with A11 antibodies rather than OC (Fig. 5*B*). These species were extremely toxic (Fig. 5*C*).

Second, we took advantage of two previously characterized mutants of NM (18), in which single residues were mutated to cysteine, G51C, and Y73C. Because NM normally contains no cysteines, these mutants allow the site-specific introduction of intermolecular crosslinks with 1, 4-bis (maleimido) butane. As previously shown, introducing such crosslinks completely prevented NM assembly (18). The crosslinked dimers of G51C (51D) and Y73C (73D) produced high fluorescence with Nile Red and reacted with A11 antibodies rather than OC (Fig. 5 *A* and *B*). Both of these species were toxic to neuroblastoma cells (Fig. 5*C*).

Discussion

Many amyloidogenic polypeptides are associated with devastating human diseases, yet others serve vital biological functions. It has recently been realized that most proteins that normally adopt a stable globular structure are also capable of forming amyloids under the right physical conditions (28), establishing that the amyloid fold is most likely an ancient and, indeed, primordial protein fold. As proteins assemble into amyloid, they populate transient oligomeric intermediates (8). We have characterized the features of oligomeric intermediates formed during the assembly of the prion-determining region (NM) of the yeast Sup35 protein, a naturally occurring, well-studied functional amyloid that is not toxic. These species share biophysical properties, and conformational-specific antibody reactivities, with oligomers formed by completely unrelated amyloidogenic polypeptides (6, 10, 12, 17, 29, 30). That a natural, functional amyloid also transitions through these same types of oligomeric intermediates points to the global importance of such transition states in amyloid assembly.

Fluorescence anisotropy, fluorescence quenching, and conformation-specific antibody reactivity allowed us to distinguish multiple oligomeric species that form during assembly. NM prion assembly can now be divided into at least four distinct phases (Fig. 6): Phase I: rapid partitioning between natively unfolded monomers and oligomeric forms that do not react with A11;

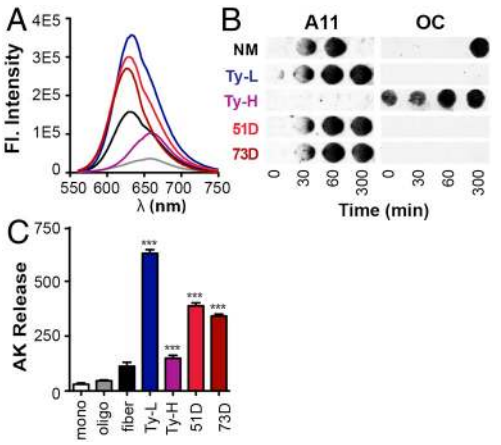

Fig. 5. Conformational features of cross-linked NM oligomers. (*A*) Nile Red binding of low molecular-weight (Ty-L, -) and high molecular weight (Ty-H, -) dityrosine crosslinked oligomers, G51C dimers (51D, -), Y73C dimers (73D, -), NM monomers (-), and NM fibers (-). (*B*) A11 and OC antibody reactivities to various oligomeric intermediates at different time points. (*C*) Toxicity of cross-linked oligomers to SH-SY5Y cells as measured by adenylate kinase release. Data are shown as mean ± SEM ($n = 3$, ***:$p < 0.001$, Dunnett's test).

Phase II: conversion of oligomers into a comformationally molten form that reacts with A11; Phase III: conformational rearrangement and compaction, with loss of A11 reactivity and the acquisition of OC reactivity in a still SDS-soluble species; Phase IV: conversion into a mature SDS-resistant amyloid. Notably, even very small quantities of A11 and OC antibodies (one molecule of antibody to approximately 80 molecules of NM) added to assembly reactions completely blocked amyloid formation. Thus, NM must transition through both A11- and OC-reactive oligomeric forms prior to assembly. That is, they are obligate, on-pathway intermediates.

To further study the properties of oligomeric intermediates formed by the yeast prion, we arrested NM in distinct oligomeric conformations using small molecules, tyrosine crosslinking, and cysteine crosslinking. We found that oligomers arrested in an OC-reactive conformation were less hydrophobic (by Nile Red binding) and were not toxic to neuroblastoma cells. Oligomers arrested in an A11-reactive conformation were more hydrophobic and were severely toxic to neuroblastoma cells. Oligomers with similar conformational-specific antibody reactivities have been previously described for a number of polypeptides associated with neurodegenerative diseases (17, 23, 30), as well as for amyloidogenic peptide fragments and proteins (10, 12, 29, 31). In those cases where it has been studied, oligomer toxicity is also associated with greater surface hydrophobicity (12, 30).

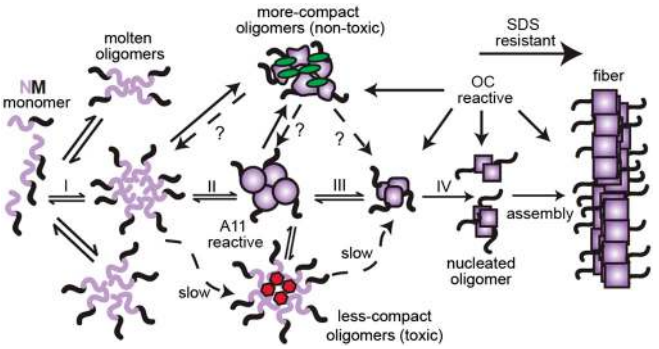

Fig. 6. NM can be arrested into four distinct conformational states. Phase I: Rapid conversion between monomers and oligomers that are not A11 reactive. Phase II: Formation of A11-reactive oligomers. Phase III: Conformational rearrangement and compaction of oligomers which are OC-reactive and still SDS soluble. Phase IV: Assembly into a mature SDS-resistant amyloid.

The question then arises: if a common toxic oligomeric conformation is critical to the assembly of both disease-associated and functional amyloids, why aren't functional amyloidogenic proteins toxic to the cells that contain them? A key feature of normal NM assembly, which sharply distinguishes it from the assembly of toxic amyloidogenic proteins, is that once the A11-reactive species appears, it converts to a nucleation-competent form that rapidly and efficiently assembles into amyloid (5). Further, propagation of the stable and self-replicating prion proceeds via a robust amyloid-templating mechanism (4). Once the amyloid forms, monomers and oligomers alike are rapidly consumed (4, 5, 14). Other functional amyloids, such as the transmembrane protein Pmel17 in melanosomes and curli in *E. coli* (31, 32), also show efficient and rapid conversion into amyloid. Hence, functional amyloids are designed to efficiently assemble into amyloid, a relatively inert protein conformation that is much less reactive with cellular constituents than the conformationally dynamic, toxic oligomers.

Selective pressures must have governed the evolution of functional amyloid sequences such that potentially toxic oligomeric intermediates are not populated for extended periods of time. What these sequence features are for yeast prions is still only beginning to be defined. For example, we recently tested 96 glutamine (Q) and asparagine (N) rich yeast protein domains (PrDs) for the capacity to form heritable, amyloid-based prions (33). Those that did were more enriched in Ns than Qs (33). Further, we studied two PrD variants of Sup35, one in which Qs were replaced by Ns, and a second in which Ns were replaced by Qs. The Q → N PrD variant assembled into amyloid with faster kinetics than the wild-type protein and was not toxic to yeast or neuroblastoma cells (34). The N → Q variant assembled extremely slowly, formed A11-reactive oligomers that existed for days, and was toxic to both yeast and neuroblastoma cells (34).

For non-functional amyloids associated with human diseases, such as Aβ and α-synuclein, assembly has not been subject to evolutionary constraints on functionality for the amyloid fold, nor selection against the toxicity of oligomers. Virtually all of the amyloid-associated diseases, including Alzheimer's and Parkinson's disease, are age related. People suffering from such disorders have only appeared in substantial numbers recently, as human life-expectancy has under gone its rapid increase. Further, the oligomers and amyloid formed by these polypeptides accumulate in biologically significant quantities after biological reproduction. Amyloid assembly is, therefore, inefficient. Toxic A11-reactive oligomers are observed both in vitro and in vivo for extended times. Moreover, assembly yields a heterogeneous population of oligomers, protofibrils, and amorphous aggregates, but relatively few fibers.

Consistent with conserved nature of the toxic oligomers that Aβ generates in humans with Alzheimer's disease, we recently found that Aβ forms oligomeric species when expressed in yeast. Moreover, the two most commonly occurring Aβ variants, Aβ 1–40 and Aβ 1–42, produce oligomers at different rates and have different toxicities in yeast, as they do in the human brain (7, 8, 35). An unbiased screen of approximately 6,000 yeast genes identified several modifiers of Aβ toxicity in yeast, and three of these were either human AD risk factors themselves or direct protein partners of risk factors (35). Those findings, taken together with results reported here, underscore the conserved nature of toxic oligomer and amyloid problems for at least a billion years of evolution.

Methods

Mutagenesis, Protein Expression and Purification. Mutagenesis, protein expression, and purification were performed according to previously reported procedures (18).

Fluorescence Experiments. Detailed experimental protocols for performing protein labeling, fluorescent quenching, anisotropy and tyrosine cross-linking are described in the *SI Text*.

ACKNOWLEDGMENTS. We thank Prof. Charles Glabe for providing A11 and OC antibodies. This work was supported by National Institutes of Health grants GM066833 to A.A.D. and GM025874 to S.L., the AvH and DFG (E.A.L.), and a National Research Service Award fellowship F32 NS067782-02 (J.L.G.).

1. Glabe CG (2008) Structural classification of toxic amyloid oligomers. *J Biol Chem* 283:29639–29643.
2. Walsh DM, et al. (1999) Amyloid beta-protein fibrillogenesis. Structure and biological activity of protofibrillar intermediates. *J Biol Chem* 274:25945–25952.
3. Harper JD, Lieber CM, Lansbury PT, Jr (1997) Atomic force microscopic imaging of seeded fibril formation and fibril branching by the Alzheimer's disease amyloid-beta protein. *Chem Biol* 4:951–959.
4. Serio TR, et al. (2000) Nucleated conformational conversion and the replication of conformational information by a prion determinant. *Science* 289:1317–1321.
5. Shorter J, Lindquist S (2004) Hsp104 catalyzes formation and elimination of self-replicating Sup35 prion conformers. *Science* 304:1793–1797.
6. Bemporad F, Chiti F (2012) Protein misfolded oligomers: Experimental approaches, mechanism of formation, and structure-toxicity relationships. *Chem Biol* 19:315–327.
7. Li S, et al. (2009) Soluble oligomers of amyloid Beta protein facilitate hippocampal long-term depression by disrupting neuronal glutamate uptake. *Neuron* 62:788–801.
8. Haass C, Selkoe DJ (2007) Soluble protein oligomers in neurodegeneration: Lessons from the Alzheimer's amyloid beta-peptide. *Nat Rev Mol Cell Biol* 8:101–112.
9. Resenberger UK, et al. (2011) The cellular prion protein mediates neurotoxic signalling of beta-sheet-rich conformers independent of prion replication. *Embo J* 30:2057–2070.
10. Bucciantini M, et al. (2002) Inherent toxicity of aggregates implies a common mechanism for protein misfolding diseases. *Nature* 416:507–511.
11. Demuro A, et al. (2005) Calcium dysregulation and membrane disruption as a ubiquitous neurotoxic mechanism of soluble amyloid oligomers. *J Biol Chem* 280:17294–17300.
12. Campioni S, et al. (2010) A causative link between the structure of aberrant protein oligomers and their toxicity. *Nat Chem Biol* 6:140–147.
13. Bieschke J, et al. (2011) Small-molecule conversion of toxic oligomers to nontoxic beta-sheet-rich amyloid fibrils. *Nat Chem Biol* 8:93–101.
14. Shorter J, Lindquist S (2005) Prions as adaptive conduits of memory and inheritance. *Nat Rev Genet* 6:435–450.
15. Halfmann R, et al. (2012) Prions are a common mechanism for phenotypic inheritance in wild yeasts. *Nature* 482:363–368.
16. Suzuki G, Shimazu N, Tanaka M (2012) A yeast prion, Mod5, promotes acquired drug resistance and cell survival under environmental stress. *Science* 336:355–359.
17. Kayed R, et al. (2003) Common structure of soluble amyloid oligomers implies common mechanism of pathogenesis. *Science* 300:486–489.
18. Krishnan R, Lindquist SL (2005) Structural insights into a yeast prion illuminate nucleation and strain diversity. *Nature* 435:765–772.
19. Mukhopadhyay S, Nayak PK, Udgaonkar JB, Krishnamoorthy G (2006) Characterization of the formation of amyloid protofibrils from barstar by mapping residue-specific fluorescence dynamics. *J Mol Biol* 358:935–942.
20. Mukhopadhyay S, Deniz AA (2007) Fluorescence from diffusing single molecules illuminates biomolecular structure and dynamics. *J Fluoresc* 17:775–783.
21. Mukhopadhyay S, Krishnan R, Lemke EA, Lindquist S, Deniz AA (2007) A natively unfolded yeast prion monomer adopts an ensemble of collapsed and rapidly fluctuating structures. *Proc Natl Acad Sci USA* 104:2649–2654.
22. Marme N, Knemeyer JP, Sauer M, Wolfrum J (2003) Inter- and intramolecular fluorescence quenching of organic dyes by tryptophan. *Bioconjug Chem* 14:1133–1139.
23. Kayed R, et al. (2007) Fibril specific, conformation dependent antibodies recognize a generic epitope common to amyloid fibrils and fibrillar oligomers that is absent in prefibrillar oligomers. *Mol Neurodegener* 2:18.
24. Feng BY, et al. (2008) Small-molecule aggregates inhibit amyloid polymerization. *Nat Chem Biol* 4:197–199.
25. Ehrnhoefer DE, et al. (2008) EGCG redirects amyloidogenic polypeptides into unstructured, off-pathway oligomers. *Nat Struct Mol Biol* 15:558–566.
26. Xi YG, Ingrosso L, Ladogana A, Masullo C, Pocchiari M (1992) Amphotericin B treatment dissociates in vivo replication of the scrapie agent from PrP accumulation. *Nature* 356:598–601.
27. Sackett DL, Wolff J (1987) Nile red as a polarity-sensitive fluorescent probe of hydrophobic protein surfaces. *Anal Biochem* 167:228–234.
28. Dobson CM (1999) Protein misfolding, evolution and disease. *Trends Biochem Sci* 24:329–332.
29. Laganowsky A, et al. (2012) Atomic view of a toxic amyloid small oligomer. *Science* 335:1228–1231.
30. Bolognesi B, et al. (2010) ANS binding reveals common features of cytotoxic amyloid species. *ACS Chem Biol* 5:735–740.
31. Wang X, Smith DR, Jones JW, Chapman MR (2007) In vitro polymerization of a functional *Escherichia coli* amyloid protein. *J Biol Chem* 282:3713–3719.
32. Fowler DM, et al. (2006) Functional amyloid formation within mammalian tissue. *PLoS Biol* 4:e6.
33. Alberti S, Halfmann R, King O, Kapila A, Lindquist S (2009) A systematic survey identifies prions and illuminates sequence features of prionogenic proteins. *Cell* 137:146–158.
34. Halfmann R, et al. (2011) Opposing effects of glutamine and asparagine govern prion formation by intrinsically disordered proteins. *Mol Cell* 43:72–84.
35. Treusch S, et al. (2011) Functional links between Abeta toxicity, endocytic trafficking, and Alzheimer's disease risk factors in yeast. *Science* 334:1241–1245.